Journal of Animal and Feed Sciences, 35, 3, 2026, e40, https://doi.org/10.22358/jafs/217223/2026
The Kielanowski Institute of Animal Physiology and Nutrition, Polish Academy of Sciences, Jabłonna

ARTICLE IN PRESS

ORIGINAL PAPER

Dietary catalpol reduces T-2 toxin-induced cartilage damage via p38MAPK/NF-κB/IAPs pathway inhibition in Wistar rats

X. Li, H. Li, L. Liu, R. He, N. Wang and K. Wang*

Harbin Medical University, Chinese Center for Disease Control and Prevention, Center for Endemic Disease Control, Harbin city, Heilongjiang Province, 150081, PR China

KEY WORDS: apoptosis, chondrocytes, dietary catalpol, NF-κB, p38MAPK, T-2 toxin

Received: 4 November 2025
Revised: 14 December 2025
Accepted: 17 December 2025

* Corresponding author:
e-mail: keweiwang957@gmail.com

ABSTRACT. This study aimed to evaluate therapeutic effects, including bactericidal and anti-inflammatory activity, inhibition of oxidative damage, neuroprotection, hepatoprotection, and suppression of hyperglycaemia. However, the protective effect of catalpol on T-2 toxin-induced cartilage damage remains unclear. The present results demonstrate that T-2 toxin causes increased chondrocyte apoptosis, leading to reduced survival of these cells. It also contributes to extracellular matrix degradation by decreasing collagen II expression and elevating matrix metalloproteinase 13 expression. Furthermore, T-2 toxin activates the p38 mitogen-activated protein kinase (p38Mapk)/nuclear factor kappa B (Nfkb)/inhibitor of apoptosis proteins (IAPs) signalling pathway and induces a dose-dependent inflammatory response in chondrocytes, reflected by elevated levels of inflammation-related mediators. Additionally, catalpol reduces T-2 toxin-induced chondrocyte apoptosis and inflammatory response by regulating the p38MAPK/NF-κB/IAPs signalling pathway. These findings elucidate the molecular mechanism underlying chondrocyte damage caused by T-2 toxin exposure and identify potential therapeutic targets, providing a theoretical basis for the use of catalpol in the treatment of T-2 toxin-induced cartilage damage.

Introduction

T-2 toxin is found in cereals and animal feed and can also be detected in livestock and poultry products, including meat, eggs, and milk (Wang et al., 2020). Human exposure through the food chain can damage multiple organs and systems in both animals and humans (Yang et al., 2022), with developing cartilage being one of its primary target tissues. In the Czech Republic, T-2 toxin was detected in up to 88% of spring barley samples (Fu et al., 2022), while in China, the contamination rate reached 79.5%, with a maximum concentration of 735 μg/kg (Li et al., 2019). Long-term consumption of grains contaminated with fungal T-2 toxin, combined with selenium deficiency, represents the main environmental risk factors for Kashin-Baker disease (KBD) (Li et al., 2019), which is characterised by extensive cartilage necrosis. KBD is an endemic disease, occurring mainly in China, Russia, and North Korea. Previous epidemiological studies have shown that the average levels of T-2 toxin in cereals from KBD-endemic regions were significantly higher than those in non-endemic areas, with concentrations in contaminated food samples ranging from 20 to 1549.4 μg/kg (mean 468.7 μg/kg) (Wang et al., 2020).

The p38 mitogen-activated protein kinase (p38MAPK) pathway plays a critical role in the regulation of cell growth, proliferation, differentiation, mitosis, gene expression, and stress responses (Ahmad et al., 2020). In mouse embryonic stem cells, exposure to T-2 toxin for 24 h resulted in a marked increase in phosphorylated p38 (p-p38)

expression and reactive oxygen species (ROS) levels (Huang et al., 2018; Chen et al., 2021). In the mouse spleen, T-2 toxin induced elevated malondialdehyde (MDA) and reactive oxygen species (ROS) levels, along with increased p-ERK/ERK, p-JNK/JNK, and p-p38/p38 ratios (Li et al., 2020a; Li and Chen, 2021; Fatima et al., 2025). This suggests that T-2 toxin triggers oxidative stress and activates the MAPK signalling cascade, ultimately leading to splenic injury. However, the involvement of the p38 MAPK signalling pathway in T-2 toxin-induced cartilage damage is unclear.

Nuclear factor kappa B (NF-κB) plays a central role in immune and inflammatory responses, as well as in cell differentiation (Abu-Amer, 2019; Afolabi et al., 2022). Active anti-inflammatory ingredients of herbal medicines have been reported to exert their effects via modulation of NF-κB activity. This factor also regulates the expression of several cytokines, including tumour necrosis factor alpha (TNF-α), and matrix metalloproteinases (MMPs) through the MAPK/NF-κB signalling pathway (Piao et al., 2019). Inhibitor of apoptosis proteins (IAPs) are a family of anti-apoptotic proteins that act by blocking caspase activation (Coyle et al., 2022). Representative members include cellular inhibitor of apoptosis protein 1 (cIAP1), cIAP2, survivin, and XIAP (Dubrez-Daloz et al., 2008; Gentle et al., 2014). There is also evidence of functional crosstalk between NF-κB and IAPs. Catalpol is a cyclic ether terpenoid with the molecular formula $C_{15}H_{22}O_{10}$, classified as a low-molecular-weight compound (Liu et al., 2007). It is one of the main active ingredients extracted from *Rehmannia glutinosa*. Animal studies have demonstrated its protective and anti-inflammatory properties in the lungs, kidneys, and heart. However, the anti-inflammatory and anti-atrophic effects of catalpol in cartilage damage in the T-2 toxin model have not yet been reported.

This study aimed to investigate alterations in the p38MAPK/NF-κB/IAPs signalling pathway following T-2 toxin induction in Wistar rats. By investigating the protective mechanism of catalpol, the present study aimed to establish a theoretical foundation for understanding and treating cartilage damage. The results demonstrate dynamic changes in TNF-α signalling and indicate that chronic inflammation selectively activates classical IAP-mediated survival pathways, including cIAP1, cIAP2, and XIAP, while suppressing survivin expression, rather than inducing a general anti-apoptotic response.

Material and methods

Animals and treatment

Wistar rats were purchased from Weitong Lihua Laboratory Animal (Beijing, China), and T-2 toxin was supplied by Pribolab Research Chemical.

Sample preparation

Urine for metabolomic analysis was collected prior to euthanasia of Wistar rats. Blood samples were collected, and knee joints were harvested and fixed in 4% paraformaldehyde for at least 48 hours. The knee joints were then decalcified in 10% ethylenediaminetetraacetic acid (EDTA), with the solution replaced every 7 days for one month (Chen et al., 2012). Following decalcification, the samples were embedded in paraffin, and whole knee joints were sectioned coronally at 5 μm thickness for further analysis.

Histopathological observation and immunohistochemistry

Tissue sections were first incubated in an oven at 58 °C for 30 min, then dewaxed and rehydrated. Sections were stained with haematoxylin and eosin (HE) and Safranin-O/Fast Green (Zhou et al., 2015). Immunohistochemical staining was subsequently performed using a collagen II antibody. In addition, histological changes were assessed according to the International Osteoarthritis Research Society (OARSI) scoring system. Cartilage histopathology was examined under a light microscope (Nikon Eclipse E200-LED, Tokyo, Japan).

TUNEL assay

The terminal deoxynucleotidyl transferase-mediated dUTP-biotin nick end labelling (TUNEL) assay was used to detect apoptosis in rat cartilage (Zhang et al., 2018). The assay was carried out using the In Situ Cell Death Detection Kit (Takara, Kyoto, Japan), following the manufacturer's instructions. Briefly, serial sagittal sections of knee joints were pretreated with 20 μg/ml protease K for 15 min, followed by inhibition with 3% hydrogen peroxide for 5 min. Terminal deoxynucleotidyl transferase was applied directly to the tissue sections for 1 h. Sections were then incubated with anti-diosgenin dioxide peroxidase antibody for 30 minutes, developed with diaminobenzidine, and counterstained with haematoxylin. Stained sections were examined under a microscope (Olympus BX53, Tokio, Japan). Image analyses were conducted with the Tanon 5500-Plus Automated Chemiluminescence Fluorescence Image Analysis System (Beijing Jitian Instru-

ment Co., Ltd., Beijing, China) and Image Pro Plus software (BD Company, Franklin Lakes, USA). The relative TUNEL positivity index was calculated as the percentage of TUNEL-positive nuclei.

Cell culture and treatment

Three to five Wistar rats (1–3 days old) were purchased from the Laboratory Animal Centre of the Second Hospital of Harbin Medical University (Harbin). Knee joints were isolated under sterile conditions and disinfected with 75% ethanol. Cartilage was cut into small pieces and digested with 0.25% trypsin for 10 min at 37 °C, followed by centrifugation at 1000 rpm for 3 min. After removing the supernatant, cartilage pieces were further digested with 2 g/l type II collagenase for 3 hours at 37 °C. The resulting cell suspension was filtered through a 70-µm cell sieve and cultured in DMEM/F12 supplemented with 10% FBS and 1% penicillin/streptomycin solution at 37 °C in 5% CO_2. The cultured cells retained general characteristic features of chondrocytes *in vivo* and were used for all experiments. For CCK8 assays, T-2 toxin concentrations were prepared at 0, 0.3, 0.6, 1.2, 2.4, 4.8, 9.6, and 19.2 ng/ml (Li et al., 2017), and catalpol concentrations at 0, 0.5, 3, 15, 75, 150, and 300 µg/ml (Cai et al., 2022).

Inhibitors used *in vivo*

The p38 MAPK inhibitor SB203580 (InvivoGen, San Diego, USA), and the NF-κB p65 inhibitor HY-18738 (InvivoGen) were used to investigate the involvement of the p38 MAPK/NF-κB signalling pathway. SB203580 was administered intraperitoneally at a dose of 0.5 mg/100 g body weight (BW) per day, and HY-18738 was administered intraperitoneally at a dose of 5 mg/100 g BW per day, as previously described (He et al., 2016; Lan et al., 2021).

Cell viability assay

Cell viability was assessed using the Cell Counting Kit-8 (CCK-8, Toshihito, Japan). Briefly, rat chondrocytes were seeded in 96-well plates. After cell attachment, they were treated with different concentrations of catalpol alone or in combination with T-2 toxin for 24 h. Subsequently, 100 µl of culture medium and 10 µl of CCK-8 reagent were added to each well, and the plates were incubated at 37 °C for 1 h. Absorbance was measured at 450 nm using a microplate reader (Cytation 3MFD; Biotek Instrument, Winooski, USA) (Chibber et al., 2021). Cell viability was calculated using the following formula: cell viability (%) = (OD treated − OD blank) / (OD control − OD blank) × 100, with control cells defined as 100% viability. Chondrocytes were exposed to increasing concentrations of T-2 toxin (0–19.2 ng/ml) for 24 h. This single time point was selected based on preliminary experiments showing that cell viability reached a plateau at 24 h, and that significant dose-dependent cytotoxicity was observed at this time. In contrast, catalpol treatment was assessed at multiple time points (12, 24, and 48 h) to determine the optimal incubation period for its protective effects.

Flow cytometry

Apoptosis rate was assessed using an Annexin V-PI double staining kit (BI, USA) in combination with flow cytometry (Becton Dickinson, Ashland, USA). Cells were seeded at a density of 1×10^6 cells per well and treated as indicated. At the end of the incubation period, cells were subjected to trypsin (cat. no. C0205; Beyotime Biotechnology, China) digestion, rinsed three times with cold phosphate-buffered saline (PBS), and then resuspended in 500 µl of binding buffer at a density of 1 × 106 cells/ml. Subsequent steps were carried out according to the manufacturer's instructions. Data were analysed using FlowJo v10 software (Becton Dickinson) (Liu et al., 2023).

Quantitative real-time PCR analysis

Total RNA was isolated from primary chondrocytes isolated from Wistar rat cartilage tissue using TRIzol reagent (Takara). RNA (2 µg) was reverse-transcribed into cDNA using the PrimeScript RT kit (Takara), according to the manufacturer's instructions. Quantitative real-time PCR was performed using the SYBR PrimeScript RT-PCR Kit II (Takara) on a Q5 real-time fluorescent quantitative PCR system (Thermo Fisher Scientific, Waltham, USA). Primer sequences for all genes are listed in Table 1. Relative mRNA expression was determined using the $2^{-\Delta\Delta Ct}$ method, with actin, beta as the internal reference gene (Piao et al., 2020).

Immunofluorescence

Chondrocytes were seeded in 6-well plates and subjected to immunofluorescent staining for type II collagen and other major proteins in the pathway. Upon reaching approximately 50% confluence, cells were treated with T-2 toxin alone or in combination with catalpol. Cells were then fixed with 4% paraformaldehyde for 15 min and washed 3 times with PBS. Subsequently, cells were permeabilised with 0.3% Triton X-100 for 10 min and blocked with 5% bovine serum albumin (BSA) overnight. The chondrocytes were then incubated with primary antibody at 4 °C overnight, rinsed with PBS and incubated with secondary antibody for 1 hour at room temperature in the dark. Finally, nuclei were counterstained with

Table 1. Primer sequences for PCR

Gene	Primer sequence (5'→3')	Gene acc. no.
Actb	F: CGTGCCACTGAAGTACCTGT	NM_001301.4
	R: GTCCCGCCAGTTCTTGAAGA	
Collagen II	F: TAGGAGTCGAGGGACCCAAG	NM_001844.6
	R: AGGCTCTCCCTTAGGACCAG	
cIAP1	F: TGCTGGACAACTGGAAACA	NM_001194437.1
	R: GAGGGCAGGCTGGAAT	
cIAP2	F: ACGGTGGGATTGCATTCCAT	NM_001309.2
	R: GCCAAGTGCAAAGGTGTCTG	
Xiap	F: TTCAGCATCAACATTGGCGC	NM_003823.3
	R: GTGTCTCCTGTGCTCTGACC	
Survivin	F: GACCTGGCAGCTGTACCTTA	NM_001168.3
	R: GCGTAAGGCAGCCAGCTG	
p65	F: ACCGGACTGACTGATGGAGA	NM_001301238.1
	R: CAGCCTCTTACCGTTCTGCA	
p38	F: AGCTGAACAAGACCGTCTGG	NM_001115263.1
	R: TTTCGTCATCAGTGTGCCGA	
Tnf	F: GATCGGTCCCAACAAGGAGG	NM_000594.3
	R: CTCCAAAGTAGACCTGCCCG	
Mmp13	F: ATGTGGAGTGCCTGATGTGG	NM_002427.6
	R: ATCAAGGGATAGGGCTGGGT	
Bax	F: AAGACAGGGGCCTTTTTGCT	NM_004324.4
	R: CCAGATGGTGAGTGAGGCAG	
Bcl2	F: GAGGGGCTACGAGTGGGATA	NM_000633.4
	R: TCAAACAGAGGTCGCATGCT	
IKBα	F: GACTCTCCACCTGCAAGACC	NM_020529.4
	R: AGCCCTGTATTCCGTCTCCT	

Actb – actin, beta, Collagen II – type II collagen, *cIAP1* – cellular inhibitor of apoptosis protein 1, *cIAP2* – cellular inhibitor of apoptosis protein 2, *Xiap* – X-linked inhibitor of apoptosis protein, Survivin – inhibitor of apoptosis protein, *p65* – nuclear factor kappa-light-chain-enhancer of activated B cells (NF-kB p65), *p38* – mitogen-activated protein kinase p38, *Tnf* – tumor necrosis factor, *Mmp13* – matrix metalloproteinase 13, *Bax* – *BCL2* associated X, apoptosis regulator, *Bcl2* – B-cell lymphoma 2, *IKBα* – inhibitor of kappa B alpha

4',6-diamidino-2-phenylindole (DAPI) for 10 min, and fluorescence signals were visualised using a fluorescence microscope (Shen et al., 2022).

Statistical analysis

Data were analysed using one-way analysis of variance (ANOVA) followed by Tukey's post hoc test. A P-value < 0.05 was considered statistically significant. All *in vitro* experiments were performed at least in triplicate. Statistical analyses were conducted using SAS 9.4 software, and quantitative plots were generated with GraphPad Prism 5 (Wang et al., 2021a).

Results

The *in vitro* experiments were performed using third-passage chondrocytes isolated from Wistar rats (Figure 1A). Primary chondrocytes showed a typical polygonal, cobblestone-like morphology (Figure 1B). Toluidine blue staining confirmed the chondrocytic phenotype (Figure 1C), and collagen II immunofluorescence further verified cell identity (Figure 1D), indicating high purity of the cultured chondrocytes.

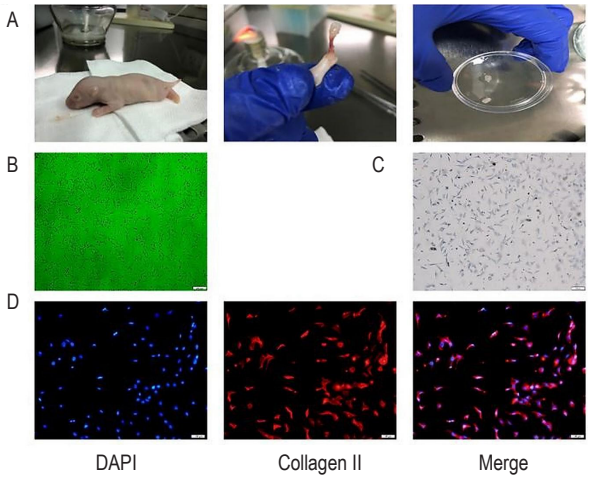

Figure 1. Morphology of primary chondrocytes with the identified result. Primary chondrocyte extraction (A). Chondrocyte microscopic morphology (scale bar = 200 μm) (B). Toluidine blue staining of chondrocytes and the number and morphology of chondrocytes were observed (scale bar = 100 μm) (C). Chondrocyte type II collagen immunofluorescence staining results (scale bar = 100 μm) (D).

Cell viability decreased progressively with increasing concentrations of T-2 toxin (Figure 2A). The half-maximal inhibitory concentration (IC_{50}) was 4.8 ng/ml, at which chondrocyte viability was reduced to 53.76%; therefore, 4.8 ng/ml was selected as the highest dose for subsequent experiments. As shown in Figure 2B, catalpol did not exert cytotoxic effects on chondrocytes within the concentration range of 0–300 μg/ml. Based on the experimental results, catalpol concentrations of 3, 15, and 75 μg/ml were selected for further *in vitro* experiments. The proliferation rate of the third-passage chondrocytes increased gradually and reached the peak at 24 h of culture, after which a marked decline was observed; accordingly, a 24 h incubation period was selected for subsequent experiments (Figure 2C).

The rate of apoptosis was significantly higher in the high-dose T-2 group than in the control group, as shown by more intensive browning in the TUNEL assay (* $P < 0.05$, ** $P < 0.01$, *** $P < 0.001$; n = 6; Figure 3A) and flow cytometric analysis (* $P < 0.05$, ** $P < 0.01$; n = 3; Figure 4A). These results were further validated by quantitative analysis of the apoptotic rate (Figure 4B). Treatment with catalpol at the concentrations indicated above significantly attenuated chondrocyte apoptosis, as shown by TUNEL staining (Figure 3B) and flow cytometry (* $P < 0.05$, ** $P < 0.01$, *** $P < 0.001$, n = 6, and * $P < 0.05$, ** $P < 0.01$, *** $P < 0.001$, n = 3, Figure 5A; B).

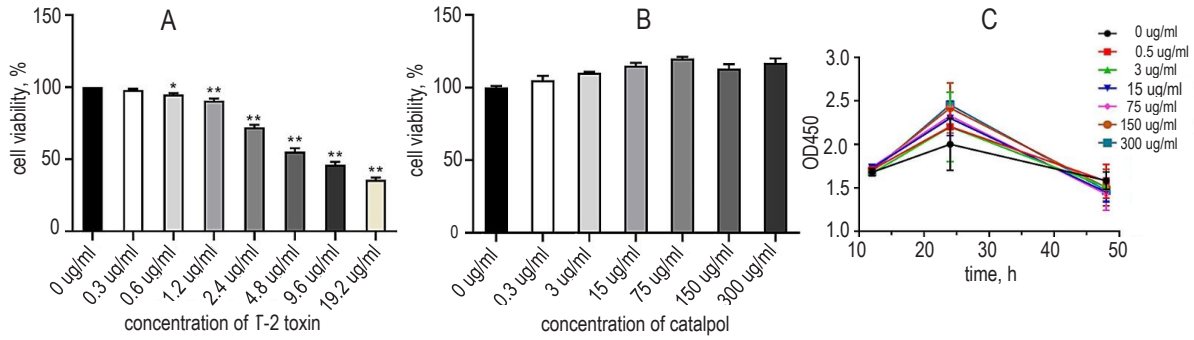

Figure 2. Data are expressed as the means ± standard deviation (SD) (A). ns, $P \geq 0.05$ vs 0 ng/ml, * $P < 0.05$ vs 0 ng/ml, ** $P < 0.01$ vs 0 ng/ml, n = 3. The effect of catalpol on chondrocyte viability (B). Data are expressed as the means ± SD. ns, $P \geq 0.05$ vs 0 ng/ml, n = 3. Catalpol at different concentrations (0–300 ug/ml) was used to determine whether there was obvious chondrocytotoxicity at 12 h, 24 h, and 48 h (C).

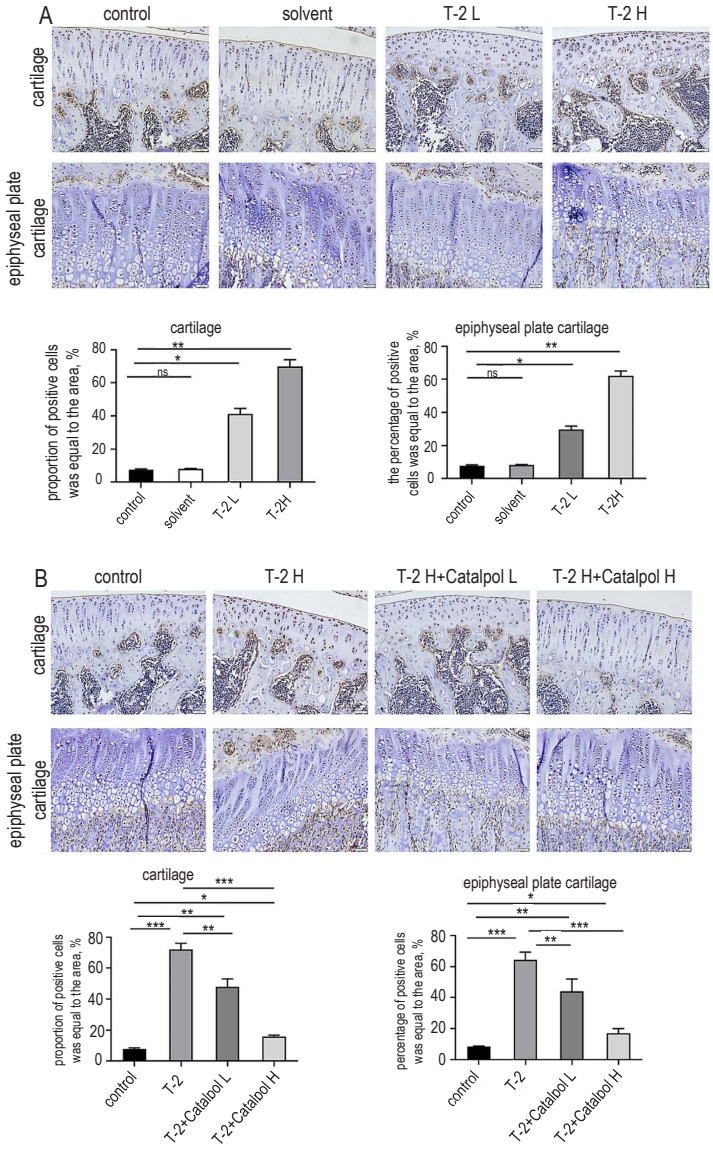

Figure 3. T-2 toxin induced chondrocyte apoptosis in Wistar rats. TUNEL staining of cartilage and epiphyseal plate cartilage was performed with increasing concentration of T-2 toxin (scale bar = 50 μm) (A). Percentage of positive staining for TUNEL in rat cartilage and epiphyseal growth plates (n = 6). Data are expressed as the means ± standard deviation (SD). ns, $P \geq 0.05$ vs Control, * $P < 0.05$ vs Control, ** $P < 0.01$ vs Control. After adding catalpol, the TUNEL staining results of cartilage and epiphyseal plate cartilage were obtained (scale bar = 50 μm) (B). Percentage of positive staining for TUNEL in rat cartilage and epiphyseal growth plates. Data are expressed as the means ± SD.* $P < 0.05$, ** $P < 0.01$, *** $P < 0.001$, n = 6.

T-2 H – high dose T-2 toxin, T-2 H+ Catalpol L – T2 toxin group treated with low dose catalpol, T-2 H + Catalpol H – T2 toxin group treated with high dose catalpol

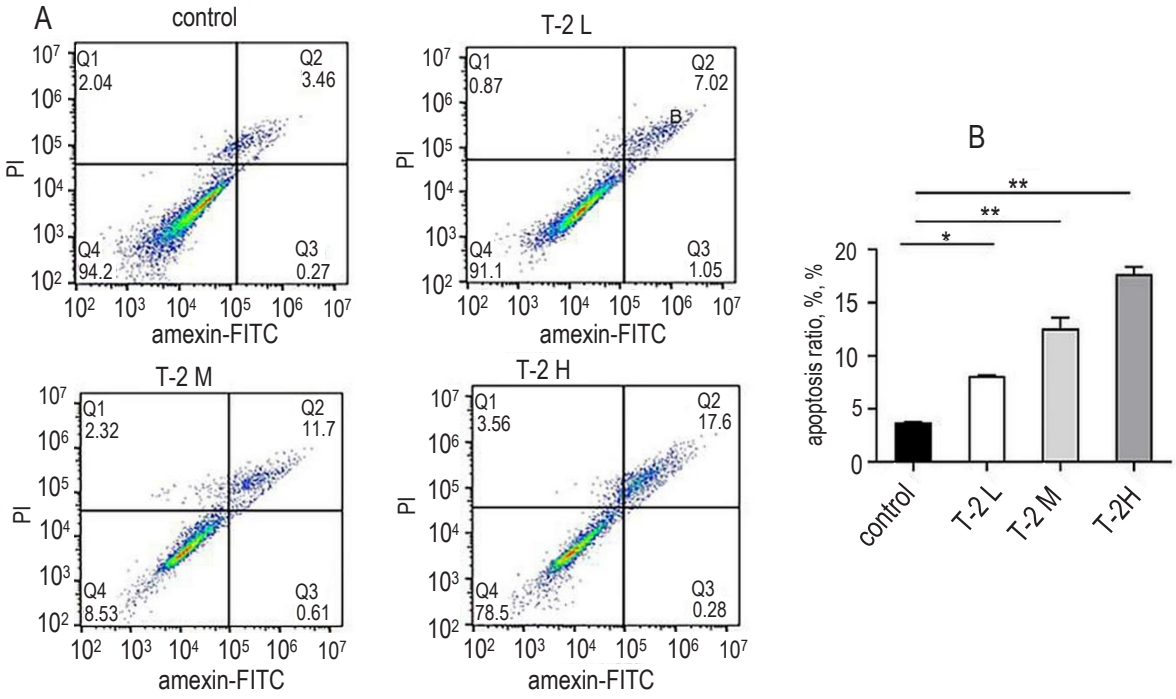

Figure 4. (A) shows the percentage of apoptotic cells of third generation chondrocytes after 24 h of treatment with T-2 toxin (0, 1.2, 2.4, and 4.8 ng/ml), respectively. The percentage of apoptotic cells in the high dose group (T-2 = 4.8 ng/ml) was significantly higher than that in the control group. Flow cytometry results showed that the apoptotic rate of chondrocytes increased with increasing concentrations of T-2 toxin. Bar chart showing the apoptotic ratio (B). Data are expressed as mean ± standard deviation. * $P < 0.05$, ** $P < 0.01$, *** $P < 0.001$ vs. Control group, n = 3, statistically significant difference.

T-2 L – low dose T2 toxin, T-2 M – medium dose T-2 toxin, T-2 H – high dose T-2 toxin

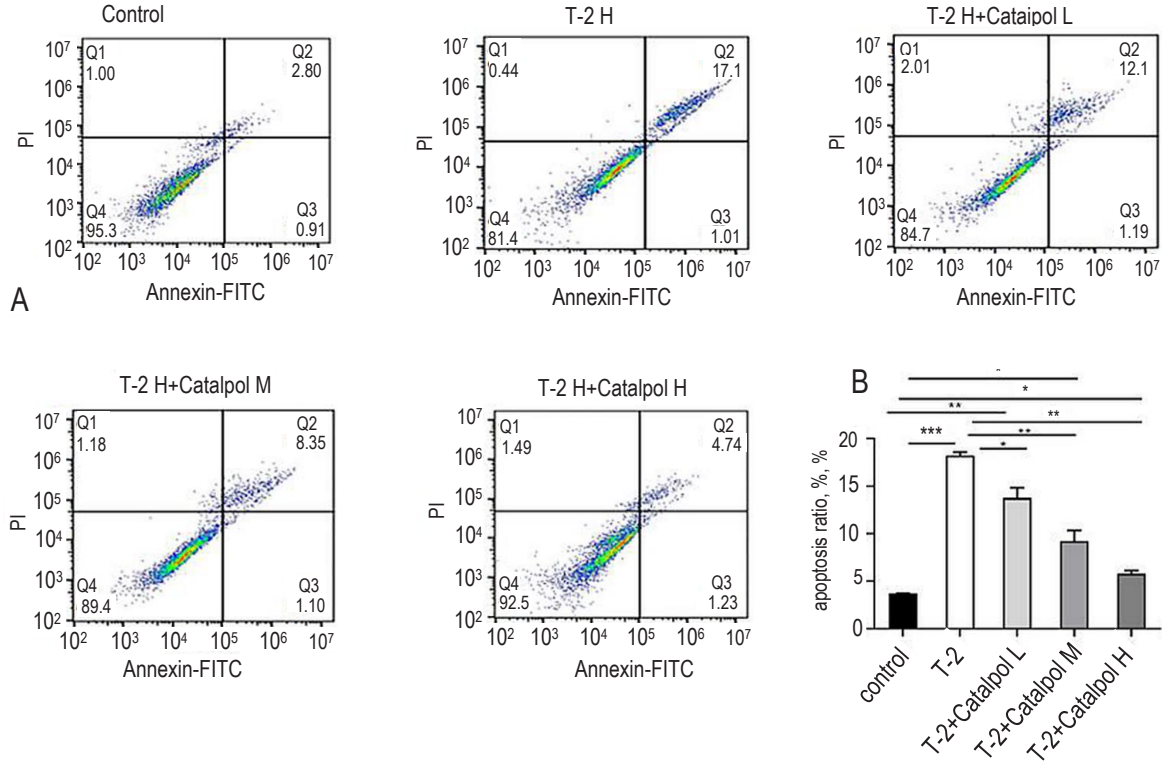

Figure 5. After adding different concentrations of catalpol, the flow cytometry was used to detect the apoptosis of chondrocytes injured by T-2 toxin. Data are expressed as the means ± standard deviation. * $P < 0.05$, ** $P < 0.01$, *** $P < 0.001$, n = 3.

T-2 H – high dose T2 toxin, T-2 H+Catalpol L – T2 toxin group treated with low dose catalpol, T-2 H+Catalpol M – T2 toxin group treated with medium dose catalpol, T-2 H+catalpol H – T2 toxin group treated with high dose catalpol

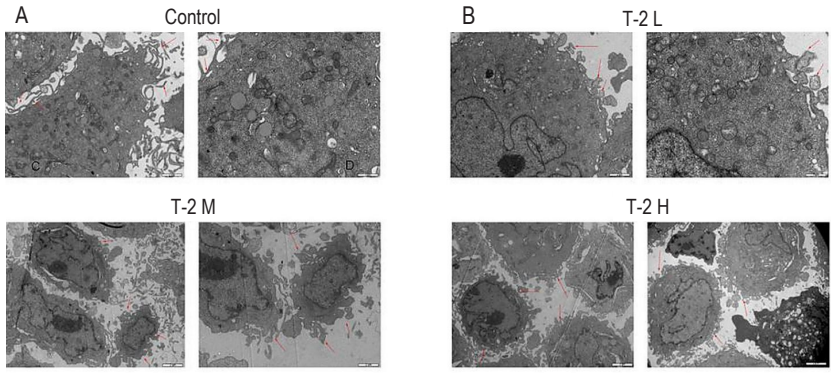

Figure 6. The ultrastructure of chondrocytes treated with different concentrations of T-2 toxin was observed (scale bar = 2 μm, scale bar = 1 μm), n = 3. (A) The normal cellular structure without exposure to T-2 toxin. The control group shows, that cells are generally intact, and there is no significant damage or disruption of organelles. (B) T-2 L shows cells exposed to a low dose of T-2 toxin. The cells have minor damage, such as minor vesicular changes, swelling, or slight structural distortions in cellular components, which are characteristic of early stages of toxicity at lower concentrations of the toxin. T-2 M represents the effect of a medium dose of T-2 toxin. The damage to the cells is pronounced compared to the T-2 L. Cells have larger vacuoles, membrane disruptions, and mitochondrial changes. These are signs of moderate toxicity affecting the cellular integrity. T-2 H – cells exposed to a high dose of T-2 toxin. More significant vacuolation, complete membrane disruption, mitochondrial swelling can be seen. These structural changes would indicate the high toxicity of T-2 toxin at elevated doses. Red arrows represent highest areas of damage at each figure.

T-2 toxin also induced marked ultrastructural alterations in chondrocytes (Figure 6), while cells in the control group had intact morphology (Figure 6A). At low T-2 concentrations, chondrocytes showed mild nuclear condensation, mitochondrial swelling, and early apoptotic changes. Moderate T-2 doses resulted in intermediate apoptotic features, characterised by cytoplasmic shrinkage and increased nuclear condensation. Exposure to high T-2 concentrations ld to late-stage apoptosis, with nuclear fragmentation, pronounced cytoplasmic reduction, and enlarged apoptotic bodies (Figure 6B).

Immunohistochemical analysis revealed collagen II expression in articular cartilage and epiphyseal plate cartilage of rats exposed to T-2 toxin. Collagen II expression was high in the control and solvent groups and decreased progressively with increasing T-2 toxin doses. The differences between the exposed groups and the control group was significant (* $P < 0.05$, ** $P < 0.01$, n = 6, scale bar = 50 μm, Figure 7).

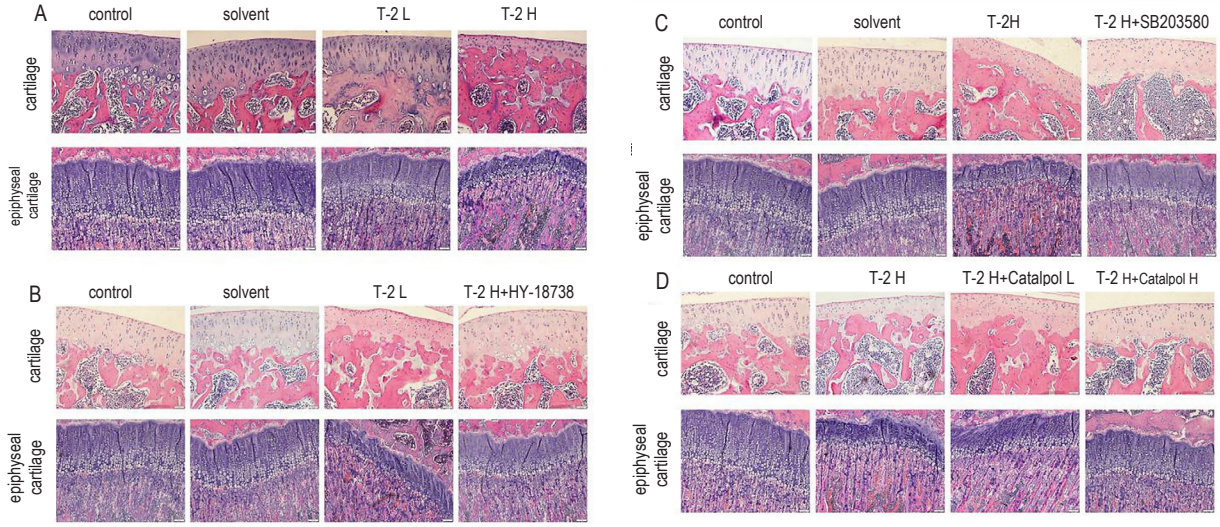

Figure 7. Histopathological changes in articular cartilage and epiphyseal plate following T-2 toxin exposure and pathway inhibition. Control group, solvent group, low-dose T-2 toxin group (0.01 mg/100 g BW/day), and high-dose T-2 toxin group (0.02 mg/100 g BW/day) (A).Control group, solvent group, high-dose T-2 toxin group, and high-dose T-2 toxin plus p38 MAPK inhibitor SB203580 group (B). Control group, solvent group, high-dose T-2 toxin group, and high-dose T-2 toxin plus NF-κB p65 inhibitor HY-18738 group (C). High-dose T-2 toxin group treated with increasing concentrations of catalpol (D). Scale bar = 50 μm and 100 μm.

T-2 L – low dose T2 toxin group, T-2 H – high dose T2 toxin, T-2 H+HY-18738 – high dose T2 toxin group treated with HY-18738, a JNK (c-Jun N-terminal kinase) inhibitor, T-2 H+SB203580 – high dose T2 toxin group treated with a selective inhibitor of p38 mitogen-activated protein kinase (p38 MAPK), T2+Catalpol L – T2 toxin group treated with low dose catalpol, T-2+catalpol H – T2 toxin group treated with high dose catalpol

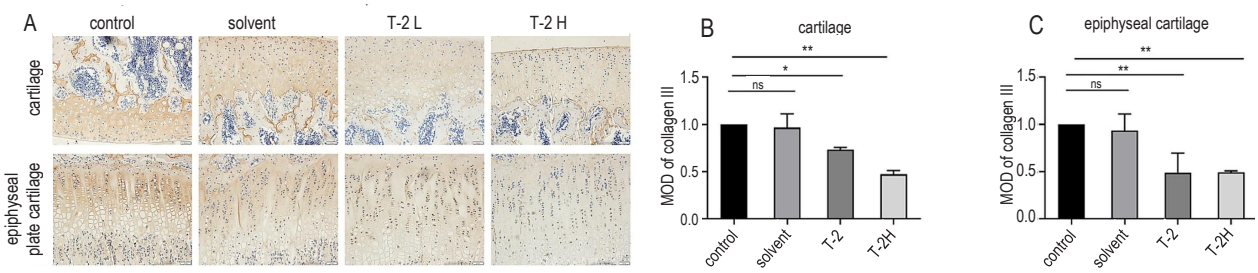

Figure 8. Immunohistochemistry was used to detect the expression of collagen II in cartilage and epiphyseal plate cartilage of rats exposed to T-2 toxin (scale bar = 50 μm; * $P < 0.05$, ** $P < 0.01$, n = 6) (A). B and C – bar chart showing mean optical density (MOD) of cartilage and epiphyseal cartilage.

T-2 L – low dose T2 toxin, T-2 H – high dose T2 toxin

The H&E staining demonstrated progressive shortening and disorganisation of the epiphyseal plate cartilage with increasing T-2 toxin doses (Figure 8A), and similar changes were observed in Safranine O/Fast green staining (Figure 9A). After the addition of p65 and p38MAPK inhibitors, both H&E and Safranine O/Fast green staining confirmed more severe damage to articular cartilage and the epiphyseal plate in the high-dose T-2 toxin group (Figure 8B; C and Figure 9B, C, respectively). In contrast, catalpol treatment reduced chondrocyte damage in a dose-dependent manner. In the high-dose catalpol group, chondrocytes showed increased thickness and more distinct stratification, and the epiphyseal plate cartilage was longer and more regularly organised than in the high-doseT-2 toxin group (Figure 8 and 9D).

In vitro cellular assay showed that treating chondrocytes with increasing concentrations of T-2 toxin (0, 1.2, 2.4, and 4.8 ng/ml) for 24 h significantly altered the expression of key signalling molecules. Analysis of mRNA and protein levels demonstrated that TNF-α stimulation induced a marked, time-dependent activation of the TAK1–NF-κB–p38 MAPK signalling axis, as evidenced by increased phosphorylation of IκBα, p65, and p38 MAPK. This activation was accompanied by robust upregulation of the anti-apoptotic mediators cIAP-1, cIAP-2, and XIAP, while survivin expression was progressively suppressed. Collectively, these findings indicate that TNF-α triggers sustained inflammatory signalling coupled with selective activation of pro-survival pathways (Figure 10).

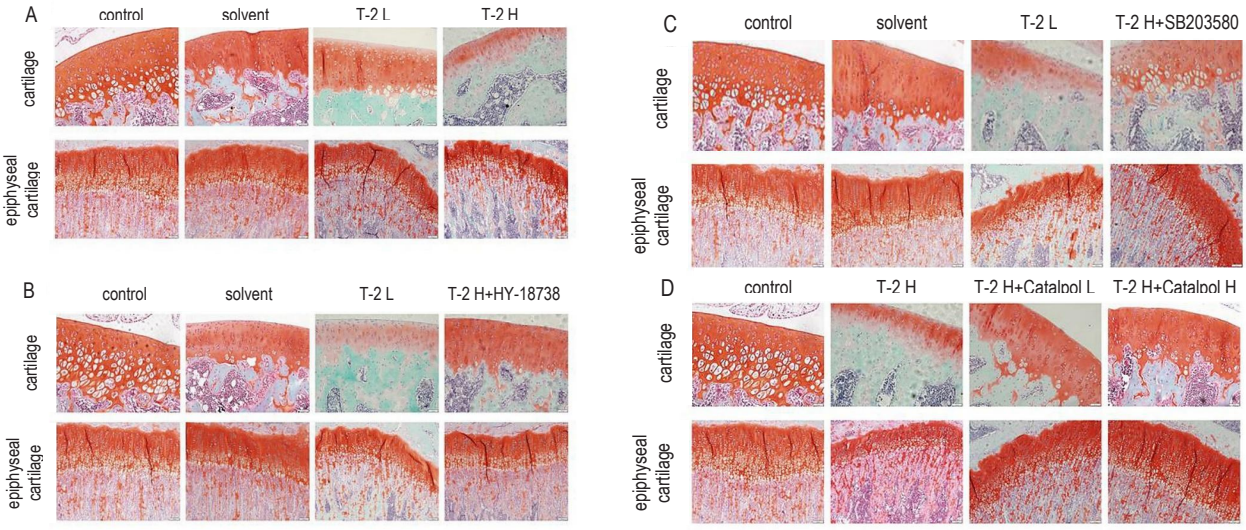

Figure 9. Pathological section results of Safranin-O-Fast green experiment in each group. Control and solvent cartilage showed lesser amounts of apoptotic cells throughout the depth of the normal cartilage. With the increase of T-2 toxin concentration, cartilage shows an amounts of apoptotic cells from superficial to middle zone of chondrocytes. When the inhibitor or catalpol was added, the injury of chondrocytes was reduced (scale bar = 50 μm, scale bar = 100 μm); n = 6. Control group, solvent group, low-dose T-2 toxin group, and high-dose T-2 toxin group (A). High-dose T-2 toxin group and high-dose T-2 toxin plus p38 MAPK inhibitor SB203580 group (B). High-dose T-2 toxin group and high-dose T-2 toxin plus NF-κB p65 inhibitor HY-18738 group (C). High-dose T-2 toxin group treated with increasing concentrations of catalpol (D).

T-2 L – low dose T2 toxin group, T-2 H – high dose T2 toxin, T-2 H+HY-18738 – high dose T2 toxin group treated with HY-18738, a JNK (c-Jun N-terminal kinase) inhibitor, T2 H+SB203580 – high dose T2 toxin group treated with a selective inhibitor of p38 mitogen-activated protein kinase (p38 MAPK), T2+Catalpol L – T2 toxin group treated with low dose catalpol, T2+catalpol H – T2 toxin group treated with high dose catalpol

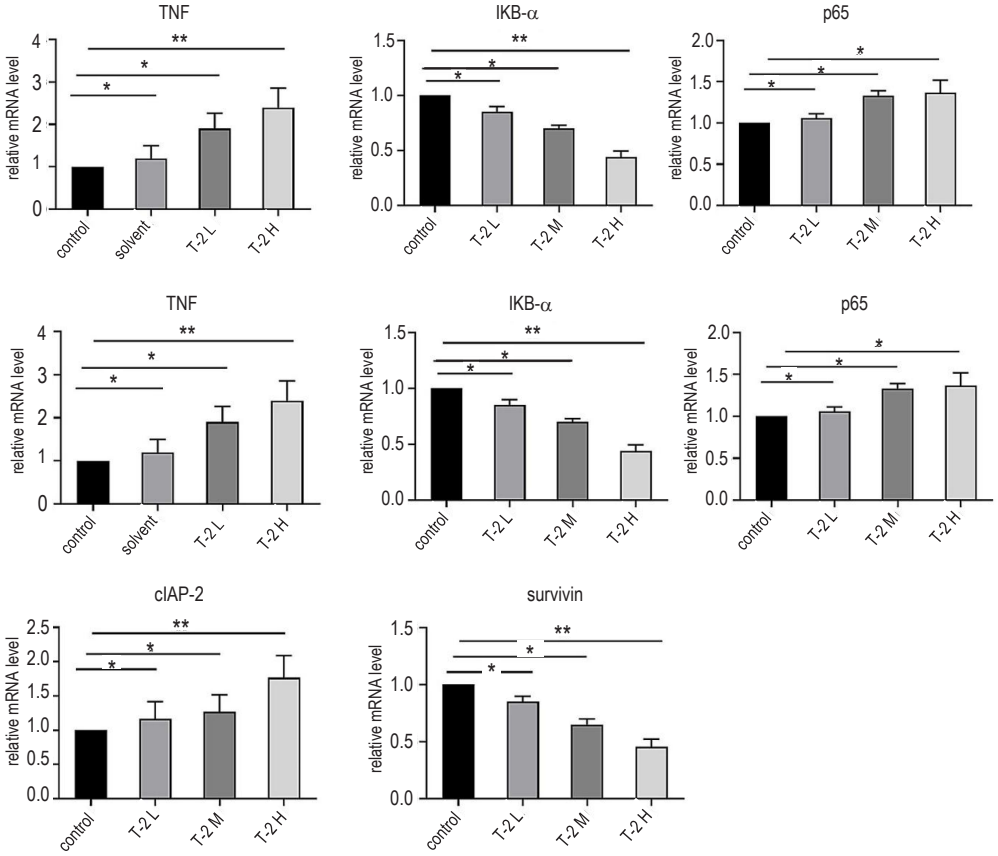

Figure 10. Effects of T-2 toxin on the expression of genes related to the p38 mitogen-activated protein kinase (*p38Mapk*)/nuclear factor kappa B (*Nfkb*)/inhibitor of apoptosis proteins (*IAP*s) signaling pathway in chondrocytes. Chondrocytes were treated with T-2 toxin (0, 1.2, 2.4, and 4.8 ng/ml) for 24 h. Data are expressed as mean ± standard deviation (n = 3). ns, $P \geq 0.05$, * $P < 0.05$, ** $P < 0.01$, *** $P < 0.001$ vs. control group.

Tnf – tumor necrosis factor, IKBα – inhibitor of kappa B-alpha, p65 – RelA (p65) subunit of NF-kB, p38 Mapk – p38 mitogen-activated protein kinase, cIAP1 – cellular inhibitor of apoptosis protein 1, Xiap – X-linked inhibitor of apoptosis protein, cIAP2 – cellular inhibitor of apoptosis protein 2, Survivin – a member of the inhibitor of apoptosis protein (IAP) family, T-2 L – low dose T2 toxin, T-2 M – medium dose T-2 toxin, T-2 H – high dose T2 toxin

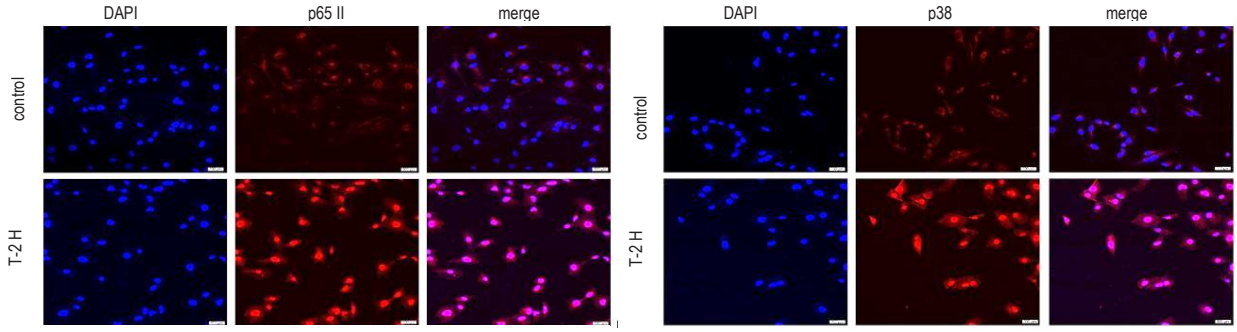

Figure 11. Immunofluorescence analysis of NF-κB p65 and p38 MAPK localization in chondrocytes following T-2 toxin exposure. T-2 toxin induced nuclear translocation of p65 and p38 compared with the control group, indicating activation of the NF-κB and p38 MAPK signaling pathways. Scale bar = 100 µm.

DAPI – 4',6-Diamidino-2-Phenylindole, p65 – RelA subunit of mNF-kB (nuclear factor kappa-light-chain-enhancer of activated B cells), T-2 H – high dose T2 toxin, p38 – p38 mitogen-activated protein kinase

Immunofluorescence analysis showed that in T-2 toxin-treated chondrocytes, p65 and p38 were initially located in the cytoplasm. High-dose T-2 toxin could have activated the NF-κB and p38 MAPK signalling pathways, resulting in increased nuclear translocation of both p65 and p38 (Figure 11). Collagen II intensity decreased progressively with increasing T-2 toxin exposure. The relative immunofluorescence intensity of collagen II was significantly higher in the control group compared to the T-2 toxin group (Figure 12, * $P < 0.05$, ** $P < 0.01$, n = 3). Treatment with catalpol protected chondrocytes from T-2-induced damage, enhancing collagen II expression in a dose-dependent manner.

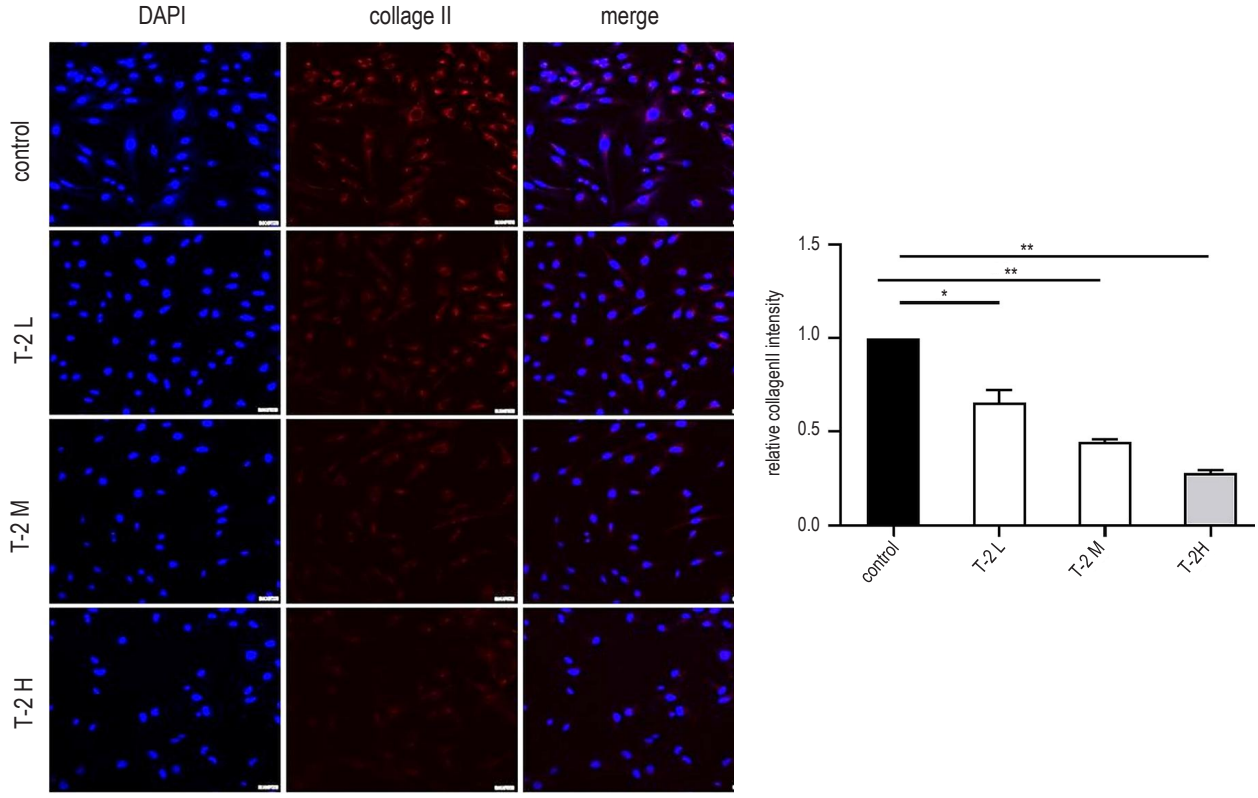

Figure 12. Immunofluorescence analysis of type II collagen (Collagen II) expression in chondrocytes treated with increasing concentrations of T-2 toxin (0, 1.2, 2.4, and 4.8 ng/ml). Quantitative analysis of relative fluorescence intensity is shown. Data are expressed as mean ± standard deviation (n = 3). * $P < 0.05$, ** $P < 0.01$ vs. control group.

T-2 L – low dose T2 toxin, T-2 M – medium dose T2 toxin, T-2 H – high dose T2 toxin

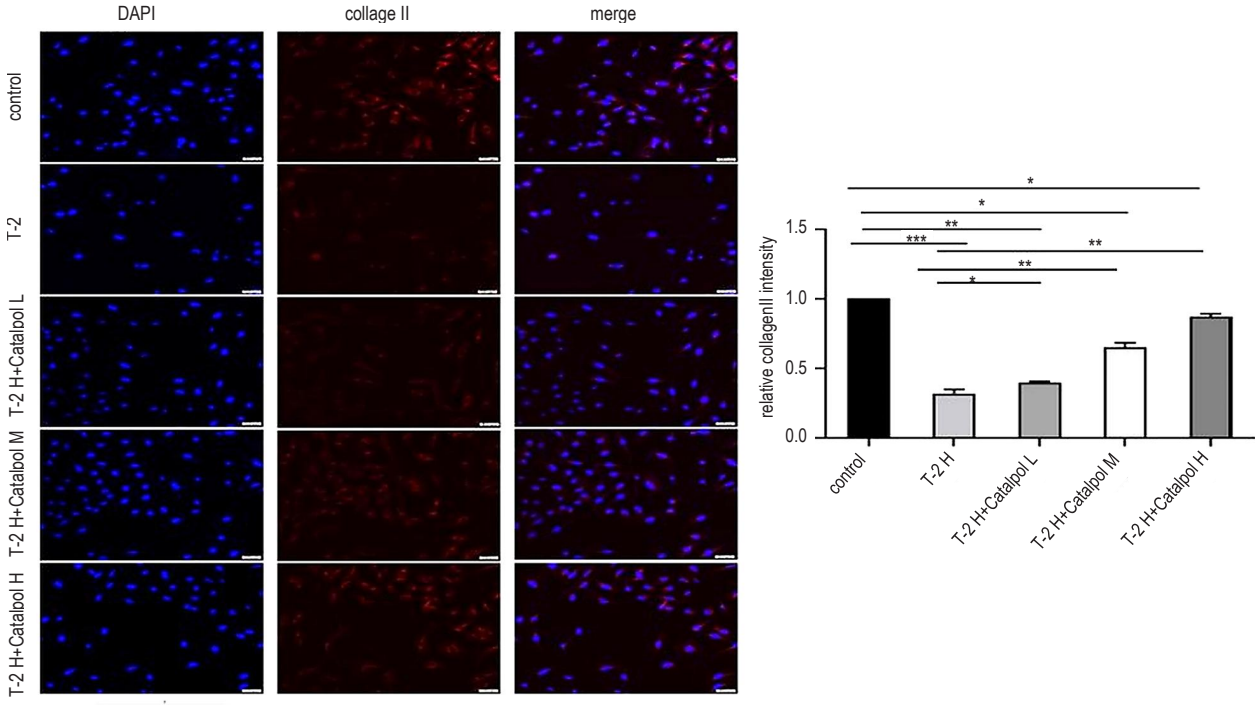

Figure 13. After adding catalpol, the results of immunofluorescence of collagen II in chondrocytes induced by T-2 were observed. The relative collagen intensity kept on increasing after increasing the catalpol concentration as validated by bar chart. (scale bar = 100 μm). Data are expressed as the means ± standard deviation.* $P < 0.05$, ** $P < 0.01$, *** $P < 0.001$, n = 3.

T-2 L – low dose T2 toxin, T-2 M – medium dose T2 toxin, T-2 H – high dose T2 toxin, T-2H+Catalpol L – low dose catalpol added to T-2 H group, T2 H+Catalpol M – medium dose of catalpol added to T-2 H group, T2H+Catalpol H – high dose of catalpol added to T-2 H group

The relative immunofluorescence intensity of collagen II increased gradually with higher catalpol concentrations compared with the high-dose T-2 group (Figure 13).

Discussion

Kashin-Beck disease (KBD) has been investigated for more than 160 years; however, its aetiology and pathogenesis remain incompletely understood. Previous studies have demonstrated that the disease is associated with excessive intake of T-2 toxin, although the mechanism underlying cartilage damage are still unclear (Wang et al., 2020; 2021a; Fu et al., 2022). Contamination of grains with T-2 toxin is considered the main cause of cartilage lesions in KBD (Li et al., 2019; Zhang et al., 2021). The primary pathological features of KBD include multiple focal necroses in deep articular cartilage, excessive chondrocyte necrosis and apoptosis, and extracellular matrix degeneration. In both humans and livestock, dietary exposure through consumption of contaminated grains represents the most common route of T-2 toxin intake (Zhang et al., 2019; 2022b). In the present study, a Wistar rat model of T-2 toxin-induced articular cartilage injury was established. The results demonstrated that T-2 toxin induced cartilage damage by inducing cell necrosis and apoptosis. Furthermore, T-2 toxin markedly accelerated the reduction of collagen II and enhanced the synthesis of matrix metalloproteinases. These findings suggest the involvement of post-transcriptional protein modifications or other complex molecular regulatory mechanisms, which require further investigations.

The MAPK signalling pathway plays a central role in regulating cellular responses to stress, including proliferation, differentiation, inflammation, and apoptosis (Qiu et al., 2022; Shi et al., 2022; Wei et al., 2022). In mammalian cells, this pathway comprises three major interconnected nodes that coordinate or modulate downstream signal transduction (Li et al., 2021; Yang et al., 2021). The NF-κB signalling pathway is a key transcriptional regulatory system involved in multiple pathophysiological processes, including immune and inflammatory responses, apoptosis, and tumorigenesis (Huang et al., 2016; Jiao et al., 2021; Hsu et al., 2022). Under resting conditions, NF-κB resides in the cytoplasm in an inactive state, bound to inhibitory proteins in a latent p50–p65 complex (Li et al., 2020b). Recent studies have demonstrated that T-2 toxin triggers strong activation of p38/MAPK signalling in chondrocytes, leading to increased apoptosis and cartilage matrix degradation, while pharmacological inhibition of this pathway significantly decreases cellular injury (Yu et al., 2023; Lu et al., 2024). However, these studies provided preliminary observations and did not fully elucidate the downstream signalling interactions or regulatory mechanisms linking p38/MAPK activation to inflammation, apoptosis, and extracellular matrix degradation in cartilage tissue.

The present study broadens these earlier findings by demonstrating that T-2 toxin robustly activates the p38/MAPK pathway in both *in vivo* and *in vitro* models of cartilage injury, accompanied by increased nuclear translocation of NF-κB and upregulation of inhibitor of apoptosis proteins (IAPs). Importantly, pharmacological inhibition of p38/MAPK or NF-κB, as well as treatment with catalpol, significantly reduced chondrocyte apoptosis, inflammatory responses, and extracellular matrix degradation. These results indicate that p38/MAPK functions as an upstream regulatory node that coordinates NF-κB/IAPs signalling in T-2 toxin-induced cartilage damage. Thus, while previous studies suggested a role for p38/MAPK activation in T-2 toxin toxicity, the present findings provide a more integrated mechanistic framework and identify catalpol as a potential therapeutic modulator of this signalling axis.

Abnormal apoptosis contributes to the pathological progression of cartilage damage. Evidence indicates that T-2 toxin can induce apoptosis (Zhang et al., 2022a; Zhang et al., 2022b). High concentrations of T-2 toxin trigger severe apoptotic responses in chondrocytes, leading to massive cell death. The inhibitor of apoptosis protein (IAP) family comprises NAIP, cellular inhibitor of apoptosis protein 1/2 (cIAP 1/2), X-linked inhibitor of apoptosis protein (XIAP), survivin, apollon, and livin (Moussata et al., 2012; Rathore et al., 2017). Livin and survivin are localised in the nucleus, whereas the remaining IAPs are mainly cytoplasmic. The cellular inhibitor of apoptosis protein 1/2 (cIAP 1/2) plays a role in signalling mediated by members of the tumour necrosis factor (TNF) receptor superfamily (Xu et al., 2019; Wu et al., 2022). These signalling cascades involve ubiquitination and phosphorylation events that ultimately activate MAPK signalling and the canonical NF-κB pathway, thereby promoting cell survival. In addition, cellular inhibitor of apoptosis protein 1/2 (cIAP 1/2) suppresses the non-classical NF-κB pathway regulated by NF-κB-inducing kinase (NIK) and supports cell survival. Among the IAP family members, X-linked inhibitor of apoptosis protein (XIAP) is considered the most potent endogenous suppressor of apoptosis. XIAP modulates NF-κB activity, MAPK-activated TGF-beta-activated kinase 1 (TAK1) signalling, and enhances nuclear translocation of the

p65 NF-κB subunit. Survivin is highly expressed in embryonic tissues and in most human cancers, but is largely absent from normal adult tissues. Increased expression of survivin and NF-κB has been reported in hepatocellular carcinoma and is associated with adverse prognostic features, including larger tumour size, cyst invasion, portal vein thrombosis, lymph node metastasis, and advanced clinical stage (Verhagen et al., 2001; Yuan et al., 2013). In the T-2 toxin-induced chondrocyte injury model, activation of the p38MAPK/NF-κB/IAPs signalling axis was observed, as reflected by increased p-p38MAPK/p38MAPK and p-p65/p65 ratios. This activation was accompanied by enhanced chondrocyte apoptosis, intensified inflammatory responses, and accelerated extracellular matrix (ECM) degradation, leading to exacerbated tissue injury. Catalpol significantly reduced the expression of inflammatory regulators, including TNF-α, and suppressed the production of matrix metalloproteinase 13 (MMP13), a key toxin-induced catabolic enzyme, while restoring collagen II expression. Moreover, catalpol effectively inhibited T-2 toxin-induced aberrant activation of the p38MAPK/NF-κB/IAPs pathway, leading to down-regulation of p-p38MAPK/p38MAPK and p-p65/p65 expression. Although the p38MAPK and NF-κB pathways have been investigated in several other disorders, data on their involvement in T-2 toxin-induced articular cartilage injury in Wistar rats, particularly in relation to apoptosis, inflammation, and phenotypic alterations, are scarce. In the current study, T-2 toxin exposure significantly increased TNF-α, pp38/p38, pp65/p65, cIAP-1/2, and XIAP levels in chondrocytes suggesting the involvement of the P38MAPK/NF-κB/IAPs signalling cascade in T-2 toxin-induced chondrocyte apoptosis.

Catalpol is an iridoid glycoside isolated from the root of *Rehmannia glutinosa*, widely used in traditional Chinese medicine (Dong and Chen, 2013; Chen et al., 2019; Du et al., 2022). Modern pharmacological studies have demonstrated that catalpol exerts multiple biological activities, including antitumour, antibacterial, antiviral, and hypoglycaemic effects (Wang et al., 2021b; 2022; Ni et al., 2023). In addition, catalpol displays anti-inflammatory, antioxidant, cardioprotective, antihyperglycaemic, and antifibrotic properties (Liu et al., 2021a; Liu et al., 2023). Significant progress has been made in elucidating the therapeutic potential of catalpol across various tissues, organs, and cells, supporting its promising clinical applications. However, studies addressing the role of catalpol in T-2 toxin-induced cartilage damage are rare, and its molecular targets in this context have not been clearly defined. Moreover, although the bioactivity and medicinal value of catalpol have been extensively investigated, its application in Kashin-Beck disease (KBD) and T-2 toxin-induced articular cartilage damage in Wistar rats has not been previously reported. In the present study, catalpol significantly reduced chondrocyte apoptosis and the expression of TNF-α, p38/p38, p65/p65, CC3/C3, Bax/Bcl-2, cIAP-1/2, and XIAP at both the protein and mRNA levels, as well as the expression of MMP13. In this study, the catabolic enzyme MMP13 was evaluated at the transcriptional level using quantitative real-time PCR rather than by protein-based assays. T-2 toxin exposure significantly upregulated *Mmp*13 mRNA expression, whereas catalpol treatment effectively reversed this effect, indicating suppression of T-2 toxin-induced extracellular matrix degradation at the transcriptional level.

Taken together, the results suggest that cartilage damage induced by T-2 toxin exposure triggers apoptosis via activation of the p38MAPK/NF-κB/IAPs pathway. Catalpol markedly attenuates this injury by modulating this signalling axis. The present study provides new information concerning the molecular mechanism of T-2 toxin-induced cartilage damage. Moreover, the evaluation of multiple catalpol concentrations demonstrates its dose-dependent protective effects on injured cartilage, offering a rationale for optimising therapeutic strategies. Collectively, these results support the potential clinical application of catalpol in the treatment of cartilage injuries.

Conclusions

T-2 toxin induces chondrocyte apoptosis, extracellular matrix degradation, and inflammation, processes that appear to be mediated by activation of the p38MAPK/NF-κB/IAPs signalling pathway. Catalpol suppressed this pathway and significantly alleviated apoptosis, inflammatory response, and extracellular matrix degradation. These findings indicate that catalpol exerts a protective effect against T-2 toxin-induced chondrocyte injury through modulation of the p38MAPK/NF-κB/IAPs axis. In conclusion, this study clarifies the molecular basis of chondrocyte apoptosis, matrix degradation, and supports the potential application of catalpol as a therapeutic agent.

Limitations

Protein-level validation of MMP13 expression using Western blotting or immunohistochemistry

was not performed, which is a limitation of the current study. This aspect should be addressed in future studies.

Funding

This study was supported by the State Administration of Foreign Experts Affairs (20172300014).

Conflict of interest

The Authors declare that there is no conflict of interest.

References

Abu-Amer Y., 2019. NF-κB mediates inflammation-induced metabolic and senescence changes in OA. Osteoarthr. Cartil. 27, S20−S21, https://doi.org/10.1016/j.joca.2019.02.028

Afolabi O.A., Anyogu D.C., Hamed M.A., Odetayo A.F., Adeyemi D.H., Akhigbe R.E., 2022. Glutamine prevents upregulation of NF-κB signaling and caspase 3 activation in ischaemia/reperfusion-induced testicular damage: An animal model. Biomed. Pharmacother. 150, 113056, https://doi.org/10.1016/j.biopha.2022.113056

Ahmad N., Ansari M.Y., Bano S., Haqqi T.M., 2020. Imperatorin suppresses IL-1 beta-induced iNOS expression via inhibiting ERK-MAPK/AP1 signaling in primary human OA chondrocytes. Int. Immunopharmacol. 85, 106612, https://doi.org/10.1016/j.intimp.2020.106612

Bhattamisra S.K., Koh H.M., Lim S.Y., Choudhury H., Pandey M., 2021. Molecular and biochemical pathways of catalpol in alleviating diabetes mellitus and its complications. Biomolecules 11, 323, https://doi.org/10.3390/biom11020323

Buhrmann C., Brockmueller A., Mueller A.L., Shayan P., Shakibaei M., 2021. Curcumin attenuates environment-derived osteoarthritis by Sox9/NF-κB signaling axis. Int. J. Mol. Sci. 22, 7645, https://doi.org/10.3390/ijms22147645

Cai C.K., Sun P.C., Chen Z.H., Sun C., Tian L.Y., 2022. Catalpol protects mouse ATDC5 chondrocytes against interleukin-1β-induced catabolism. Histol. Histopathol. 37, 333−344, https://doi.org/10.14670/HH-18-575

Chen C.J., Chen Z., Xu F., Zhu C., Fang F.F., Shu S., Li M., Ling C.Q., 2013. Radio-protective effect of catalpol in cultured cells and mice. J. Radiat. Res. 54, 76−82, https://doi.org/10.1093/jrr/rrs080

Chen D., Guo J., Li L.G., 2022. Catalpol promotes mitochondrial biogenesis in chondrocytes. Arch. Physiol. Biochem. 128, 802−808, https://doi.org/10.1080/13813455.2020.1727927

Chen H., Deng C., Meng Z., Meng S., 2022. Effects of catalpol on Alzheimer's disease and its mechanisms. Evid. Based Complement. Alternat. Med. 2022, 2794243, https://doi.org/10.1155/2022/2794243

Chen J.H., Xue S.H., Li S.Y., Wang Z.L., Yang H.J., Wang W., Song D.Q., Zhou X.R., Chen C., 2012. Oxidant damage in Kashin-Beck disease and a rat Kashin-Beck disease model by employing T-2 toxin treatment under selenium deficient conditions. J. Orthop. Res. 30, 1229−1237, https://doi.org/10.1002/jor.22073

Chen Y., Liu Q.P., Shan Z.F., Mi W.Y., Zhao Y.Y., Li M., Wang B.Y., Zheng X.K., Feng W.S., 2019. Catalpol ameliorates podocyte injury by stabilizing cytoskeleton and enhancing autophagy in diabetic nephropathy. Front. Pharmacol. 10, 1477, https://doi.org/10.3389/fphar.2019.01477

Chen Y.Y., Yan X.J., Jiang X.H., Lu F.L., Yang X.R., Li D.P., 2021. Vicenin 3 ameliorates ECM degradation by regulating the MAPK pathway in SW1353 chondrocytes. Exp. Ther. Med. 22, 1461, https://doi.org/10.3892/etm.2021.10896

Chibber P., Haq S.A., Kumar A., Kumar C., Gupta D., Wazir P., Singh S., Abdullah S.T., Singh G., 2021. Antiarthritic activity of OA-DHZ; a gastroprotective NF-κB/MAPK/COX inhibitor. Cytokine 148, 155688, https://doi.org/10.1016/j.cyto.2021.155688

Coyle R., O'Sullivan M.J., Zisterer D.M., 2022. Targeting inhibitor of apoptosis proteins (IAPs) with IAP inhibitors sensitises malignant rhabdoid tumour cells to cisplatin. Cancer Treat. Res. Commun. 32, 100579, https://doi.org/10.1016/j.ctarc.2022.100579

Deng H., Chilufya M.M., Liu J. et al., 2021. Effect of low nutrition and T-2 toxin on C28/I2 chondrocytes cell line and chondroitin sulfate-modifying sulfotransferases. Cartilage 13, 818S−825S, https://doi.org/10.1177/19476035211023555

Dong Z., Chen C.X., 2013. Effect of catalpol on diabetic nephropathy in rats. Phytomedicine 20, 1023−1029, https://doi.org/10.1016/j.phymed.2013.04.007

Du J., Liu J., Huang X., Li Y., Song D., Li Q., Lin J., Li B., Li L., 2022. Catalpol ameliorates neurotoxicity in N2a/APP695swe cells and APP/PS1 transgenic mice. Neurotox. Res. 40, 961−972, https://doi.org/10.1007/s12640-022-00524-4

Dubrez-Daloz L., Dupoux A., Cartier J., 2008. IAPs: more than just inhibitors of apoptosis proteins. Cell Cycle 7, 1036−1046, https://doi.org/10.4161/cc.7.8.5783

Fang C., Liu J., Feng M. et al., 2022. Shengyu decoction treating vascular cognitive impairment by promoting AKT/HIF-1α/VEGF-related cerebrovascular generation and ameliorating MAPK/NF-κB-mediated neuroinflammation. J. Ethnopharmacol. 296, 115441, https://doi.org/10.1016/j.jep.2022.115441

Fatima S., Abrar M., Shahid A., Moin H., Majeed S., 2025. Serum asprosin and its association with bone mineral density, oxidative stress, and osteoprotegerin levels in Pakistani women with postmenopausal osteoporosis. Expert Rev. Endocrinol. Metab. 20, 427−439, https://doi.org/10.1080/17446651.2025.2510595

Feng S., Zou L., Wang H., He R., Liu K., Zhu H., 2018. RhoA/ROCK-2 pathway inhibition and tight junction protein upregulation by catalpol suppresses lipopolysaccharide-induced disruption of blood-brain barrier permeability. Molecules 23, 2371, https://doi.org/10.3390/molecules23092371

Fu G.T., Chen X.Q., Qi M., Du X.P., Xia Z.R., Liu Q.L., Sun N., Shi C.D., Zhang R.Q., 2022. Status and potential diagnostic roles of essential trace elements in Kashin-Beck disease patients. J. Trace Elem. Med. Biol. 69, 126880, https://doi.org/10.1016/j.jtemb.2021.126880

Gentle I.E., Moelter I., Lechler N., Bambach S., Vucikuja S., Häcker G., Aichele P., 2014. Inhibitors of apoptosis proteins (IAPs) are required for effective T-cell expansion/survival during antiviral immunity in mice. Blood 123, 659−668, https://doi.org/10.1182/blood-2013-01-479543

He B., Tao H.Y., Liu S.Q., Wei A.L., Pan F., Chen R., Li X.H., 2016. Carboxymethylated chitosan protects rat chondrocytes from NO-induced apoptosis via inhibition of the p38/MAPK signaling pathway. Mol. Med. Rep. 13, 2151−2158, https://doi.org/10.3892/mmr.2016.4772

He Y., Shi Y., Zhang Y., Zhang R., Cao L., Liu Y., Ma T., Chen J., 2023. T-2 toxin-induced chondrocyte apoptosis contributes to growth plate damage through Smad2 and Smad3 signaling. Toxicon 232, 107193, https://doi.org/10.1016/j.toxicon.2023.107193

Hong H., Lou S., Zheng F., Gao H., Wang N., Tian S., Huang G., Zhao H., 2022. Hydnocarpin D attenuates lipopolysaccharide-induced acute lung injury via MAPK/NF-κB and Keap1/Nrf2/HO-1 pathway. Phytomedicine 101, 154143, https://doi.org/10.1016/j.phymed.2022.154143

Hsu H.C., Ke Y.L., Lai Y.H., Hsieh W.C., Lin C.H., Huang S.S., Peng J.Y., Chen C.H., 2022. Chondroitin sulfate enhances proliferation and migration via inducing beta-catenin and intracellular ROS as well as suppressing metalloproteinases through Akt/NF-κB pathway inhibition in human chondrocytes. J. Nutr. Health Aging 26, 307−313, https://doi.org/10.1007/s12603-022-1752-5

Huang D.G., Zhao Q.L., Liu H.F., Guo Y.J., Xu H.G., 2016. PPAR-alpha agonist WY-14643 inhibits LPS-induced inflammation in synovial fibroblasts via NF-κB pathway. J. Mol. Neurosci. 59, 544−553, https://doi.org/10.1007/s12031-016-0775-y

Huang X.J., Pan Q.Y., Mao Z.K., Zhang R., Ma X.H., Xi Y., You H.B., 2018. Sinapic acid inhibits the IL-1 beta-induced inflammation via MAPK downregulation in rat chondrocytes. Inflammation 41, 562−568, https://doi.org/10.1007/s10753-017-0712-4

Jiao B., Guo S.M., Yang X.H. et al., 2021. The role of HMGB1 on TDI-induced NLPR3 inflammasome activation via ROS/NF-κB pathway in HBE cells. Int. Immunopharmacol. 98, https://doi.org/10.1016/j.intimp.2021.107859

Khan S., Simpson J., Lynch J.C., Turay D., Mirshahidi S., Gonda A., Sanchez T.W., Casiano C.A., Wall N.R., 2017. Racial differences in the expression of inhibitors of apoptosis (IAP) proteins in extracellular vesicles (EV) from prostate cancer patients. PLoS One 12, e0183122, https://doi.org/10.1371/journal.pone.0183122

LaCasse E.C., Baird S., Korneluk R.G., MacKenzie A.E., 1998. The inhibitors of apoptosis (IAPs) and their emerging role in cancer. Oncogene 17, 3247−3259, https://doi.org/10.1038/sj.onc.1202569

Lan C.N., Cai W.J., Shi J., Yi Z.J., 2021. MAPK inhibitors protect against early-stage osteoarthritis by activating autophagy. Mol. Med. Rep. 24, 829, https://doi.org/10.3892/mmr.2021.12469

Li B., Wang M., Chen S. et al., 2022. Baicalin mitigates the neuroinflammation through the TLR4/MyD88/NF-κB and MAPK pathways in LPS-stimulated BV-2 microglia. Biomed. Res. Int. 2022, 3263446, https://doi.org/10.1155/2022/3263446

Li X.H., Zhang Z.L., Liang W.N. et al., 2020a. Tougu Xiaotong capsules may inhibit p38 MAPK pathway-mediated inflammation: in vivo and in vitro verification. J. Ethnopharmacol. 249, 112390, https://doi.org/10.1016/j.jep.2019.112390

Li Y., Mo X., Xiong Y., 2019. The study on polymorphism of TrxR and Nrf2/HO-1 signaling pathway in Kaschin-Beck disease. Biol. Trace Elem. Res. 190, 303−308, https://doi.org/10.1007/s12011-018-1566-9

Li Y., Zou N., Wang J., Wang K.W., Li F.Y., Chen F.X., Sun B.Y., Sun D.J., 2017. TGF-β1/Smad3 signaling pathway mediates T-2 toxin-induced decrease of type II collagen in cultured rat chondrocytes. Toxins (Basel) 9, 359, https://doi.org/10.3390/toxins9110359

Li Y.Z., Yang Y.X., Guo J.W., Guo X.J., Feng Z.Y., Zhao X.L., 2020b. Spinal NF-κB upregulation contributes to hyperalgesia in a rat model of advanced osteoarthritis. Mol. Pain 16, https://doi.org/10.1177/1744806920905691

Li Z.N., Chen B.J., 2021. DUSP4 alleviates LPS-induced chondrocyte injury in knee osteoarthritis via the MAPK signaling pathway. Exp. Ther. Med. 22, 1401, https://doi.org/10.3892/etm.2021.10837

Lin C.M., Wang B.W., Fang W.J., Pan C.M., Shyu K.G., Hou S.W., 2019. Catalpol ameliorates neointimal hyperplasia in diabetic rats. Planta Med. 85, 406−411, https://doi.org/10.1055/a-0818-3689

Lin X., Shao W., Yu F., Xing K., Liu H., Zhang F., Goldring M.B., Lammi M.J., Guo X., 2019. Individual and combined toxicity of T-2 toxin and deoxynivalenol on human C-28/I2 and rat primary chondrocytes. J. Appl. Toxicol. 39, 343−353, https://doi.org/10.1002/jat.3725

Liu A., Zhang B., Zhao W., Tu Y., Wang Q., Li J., 2021a. Catalpol ameliorates psoriasis-like phenotypes via SIRT1 mediated suppression of NF-κB and MAPKs signaling pathways. Bioengineered 12, 183−195, https://doi.org/10.1080/21655979.2020.1863015

Liu J., Wu N., Ma L.N., Zhong J.T., Liu G., Zheng L.H., Lin X.K., 2014. p38MAPK signaling mediates mitochondrial apoptosis in cancer cells induced by oleanolic acid. Asian Pac. J. Cancer Prev. 15, 4519−4525, https://doi.org/10.7314/APJCP.2014.15.11.4519

Liu J.Y., Liu S., Yu M.Y., Li J.N., Xie Z.X., Gao B.Y., Liu Y.Y., 2023. Anti-inflammatory effect and mechanism of catalpol in various inflammatory diseases. Drug Dev. Res. 84, 1376−1394, https://doi.org/10.1002/ddr.22096

Liu L.L., Zhang H., Jin B.M., Li H.N., Zheng X.J., Li X.Y., Li M.Y., Li M.Q., Nian S.J., Wang K.W., 2023. MiR-214-3p may alleviate T-2 toxin-induced chondrocyte apoptosis and matrix degradation by regulating NF-κB signaling pathway in vitro. Toxicon 225, 107049, https://doi.org/10.1016/j.toxicon.2023.107049

Liu S.L., Kong Y.F., Cai J.T., Dong C.H., 2021a. Advances in structural modification and pharmacological activity of catalpol and its derivatives. ChemistrySelect 6, 13520−13535, https://doi.org/10.1002/slct.202103380

Liu Y.N., Mu Y.D., Wang H., Zhang M., Shi Y.W., Mi G., Peng L.X., Chen J.H., 2021b. Endoplasmic reticulum stress pathway mediates T-2 toxin-induced chondrocyte apoptosis. Toxicol. 464, 152989, https://doi.org/10.1016/j.tox.2021.152989

Lu C., Yang W., Chu F. et al., 2024. Hesperetin attenuates T-2 toxin-induced chondrocyte injury by inhibiting the p38 MAPK signaling pathway. Nutrients 16, 3107, https://doi.org/10.3390/nu16183107

Moussata D., Amara S., Siddeek B. et al., 2012. XIAP as a radio resistance factor and prognostic marker for radiotherapy in human rectal adenocarcinoma. Am. J. Pathol. 181, 1271−1278, https://doi.org/10.1016/j.ajpath.2012.06.029

Ni H.B., Rui Q., Kan X.G., Gao R., Zhang L., Zhang B.L., 2023. Catalpol ameliorates oxidative stress and neuroinflammation after traumatic brain injury in rats. Neurochem. Res. 48, 681−695, https://doi.org/10.1007/s11064-022-03796-6

Piao S., Du W., Wei Y.L., Yang Y., Feng X.Y., Bai L.H., 2020. Protectin DX attenuates IL-1β-induced inflammation via the AMPK/NF-κB pathway in chondrocytes and ameliorates osteoarthritis progression in a rat model. Int. Immunopharmacol. 78, 106043, https://doi.org/10.1016/j.intimp.2019.106043

Qiu J.X., Jiang T., Yang G.Y., Gong Y.H., Zhang W.K., Zheng X.H., Hong Z.H., Chen H.X., 2022. Neratinib exerts dual effects on cartilage degradation and osteoclast production in osteoarthritis by inhibiting the activation of the MAPK/NF-κB signaling pathways. Biochem. Pharmacol. 205, 115155, https://doi.org/10.1016/j.bcp.2022.115155

Rathore R., McCallum J.E., Varghese E., Florea A.M., Büsselberg D., 2017. Overcoming chemotherapy drug resistance by targeting inhibitors of apoptosis proteins (IAPs). Apoptosis 22, 898−919, https://doi.org/10.1007/s10495-017-1375-1

Saito T., Tanaka S., 2017. Molecular mechanisms underlying osteoarthritis development: Notch and NF-κB. Arthritis Res. Ther. 19, 94, https://doi.org/10.1186/s13075-017-1296-y

Shen Y., Teng L., Qu Y.H., Liu J., Zhu X.D., Chen S., Yang L.F., Huang Y.H., Song Q., Fu Q., 2022. Anti-proliferation and anti-inflammation effects of corilagin in rheumatoid arthritis by downregulating NF-κB and MAPK signaling pathways. J. Ethnopharmacol. 284, 114791, https://doi.org/10.1016/j.jep.2021.114791

Shi M., He Y., Zhang Y., Guo X., Lin J., Wang W., Chen J., 2021a. LncRNA MIAT regulated by selenium and T-2 toxin increases NF-κB-p65 activation, promoting the progress of Kashin-Beck disease. Hum. Exp. Toxicol. 40, 869−881, https://doi.org/10.1177/0960327120975122

Shi T., Fu X., Wang F., Zhang X., Cai Y., Wu X., Sun L., 2021b. The WNT/β-catenin signalling pathway induces chondrocyte apoptosis in the cartilage injury caused by T-2 toxin in rats. Toxicon 204, 14−20, https://doi.org/10.1016/j.toxicon.2021.11.003

Shi Y.F., Chen J.X., Li S.L. et al., 2022. Tangeretin suppresses osteoarthritis progression via the Nrf2/NF-κB and MAPK/NF-κB signaling pathways. Phytomedicine 98, https://doi.org/10.1016/j.phymed.2022.153928

Verhagen A.M., Coulson E.J., Vaux D.L., 2001. Inhibitor of apoptosis proteins and their relatives: IAPs and other BIRPs. Genome Biol. 2, 3009.1, https://doi.org/10.1186/gb-2001-2-7-reviews3009

Wang H.J., Ran H.F., Yin Y. et al., 2022. Catalpol improves impaired neurovascular unit in ischemic stroke rats via enhancing VEGF-PI3K/AKT and VEGF-MEK1/2/ERK1/2 signaling. Acta Pharmacol. Sin. 43, 1670−1685, https://doi.org/10.1038/s41401-021-00803-4

Wang J., Wang X.Y., Li H.R., Yang L.S., Li Y.C., Kong C., 2021a. Spatial distribution and determinants of health loss from Kashin-Beck disease in Bin County, Shaanxi Province, China. BMC Public Health 21, 387, https://doi.org/10.1186/s12889-021-10407-6

Wang K., Yu J., Liu H., Liu Y., Liu N., Cao Y., Zhang X., Sun D., 2020. Endemic Kashin-Beck disease: a food-sourced osteoarthropathy. Semin. Arthritis Rheum. 50, 366−372, https://doi.org/10.1016/j.semarthrit.2019.07.014

Wang M., Xue S., Fang Q., Zhang M., He Y., Zhang Y., Lammi M.J., Cao J., Chen J., 2019. Expression and localization of the small proteoglycans decorin and biglycan in articular cartilage of Kashin-Beck disease and rats induced by T-2 toxin and selenium deficiency. Glycoconj. J. 36, 451−459, https://doi.org/10.1007/s10719-019-09889-9

Wang Y.L., Wu H.R., Zhang S.S., Xiao H.L., Yu J., Ma Y.Y., Zhang Y.D., Liu Q., 2021b. Catalpol ameliorates depressive-like behaviors in CUMS mice via oxidative stress-mediated NLRP3 inflammasome and neuroinflammation. Transl. Psychiatry 11, 353, https://doi.org/10.1038/s41398-021-01468-7

Wei J., Gao C., Hu K., Li M.Y., Li J.S., Shen M.M., Zhang S.Y., 2022. Knockdown of DAPK1 attenuates IL-1 beta-induced extracellular matrix degradation and inflammatory response in osteoarthritis chondrocytes via regulating the p38 MAPK-signaling pathway. Allergol. Immunopathol. 50, 169−175, https://doi.org/10.15586/aei.v50i6.744

Wu Y., Lu S., Huang X., Liu Y., Huang K., Liu Z., Xu W., Zhu W., Hou J., Liu H., Zhang X., 2022. Targeting cIAPs attenuates CCl4-induced liver fibrosis by increasing MMP9 expression derived from neutrophils. Life Sci. 289, 120235, https://doi.org/10.1016/j.lfs.2021.120235

Xia T.T., Zhao R.Z., He S.J., Wang L., Fu X.J., Zhao Y., Qiao S.G., An J.Z., 2023. Gardenoside ameliorates inflammation and inhibits ECM degradation in IL-1b-treated rat chondrocytes via suppressing NF-κB signaling pathways. Biochem. Biophys. Res. Commun. 640, 164−172, https://doi.org/10.1016/j.bbrc.2022.12.016

Xu J., Hua X., Yang R., Jin H., Li J., Zhu J., Tian Z., Huang M., Jiang G., Huang H., Huang C., 2019. XIAP interaction with E2F1 and Sp1 via its BIR2 and BIR3 domains specifically activates MMP2 to promote bladder cancer invasion. Oncogenesis 8, 71, https://doi.org/10.1038/s41389-019-0181-8

Yang H.J., Zhang Y., Wang Z.L. et al., 2017. Increased chondrocyte apoptosis in Kashin-Beck disease and rats induced by T-2 toxin and selenium deficiency. Biomed. Environ. Sci. 30, 351−362, https://doi.org/10.3967/bes2017.046

Yang J., Li H., Zhang C., Zhou Y., 2022. Indoxyl sulfate reduces Ito,f by activating ROS/MAPK and NF-κB signaling pathways. JCI Insight 7, 45475, https://doi.org/10.1172/jci.insight.145475

Yang X., Zhou Y.F., Chen Z.Q., 2021. Curcumenol mitigates chondrocyte inflammation by inhibiting the NF-κB and MAPK pathways, and ameliorates DMM-induced OA in mice. Int. J. Mol. Med. 48, 192, https://doi.org/10.3892/ijmm.2021.5025

Yu F.F., Yu S.Y., Sun L. et al., 2023. T-2 toxin induces mitochondrial dysfunction in chondrocytes via the p53-cyclophilin D pathway. J. Hazard. Mater. 133090, https://doi.org/10.1016/j.jhazmat.2023.133090

Yuan Z., Syrkin G., Adem A. et al., 2013. Blockade of inhibitors of apoptosis (IAPs) in combination with tumor-targeted delivery of tumor necrosis factor-α leads to synergistic antitumor activity. Cancer Gene Ther. 20, 46−56, https://doi.org/10.1038/cgt.2012.83

Zhang F., Lammi M.J., Shao W., Zhang P., Zhang Y., Wei H., Guo X., 2019. Cytotoxic properties of HT-2 toxin in human chondrocytes: could T3 inhibit toxicity of HT-2? Toxins (Basel) 11, 667, https://doi.org/10.3390/toxins11110667

Zhang J., Song M., Cui Y., Shao B., Zhang X., Cao Z., Li Y., 2022a. T-2 toxin-induced femur lesion is accompanied by autophagy and apoptosis associated with Wnt/β-catenin signaling in mice. Environ. Toxicol. 37, 1653−1661, https://doi.org/10.1002/tox.23514

Zhang M., Wang M., Wang H. et al., 2021. Decreased expression of heat shock protein 47 is associated with T-2 toxin and low selenium-induced matrix degradation in cartilages of Kashin-Beck disease. Biol. Trace Elem. Res. 199, 944−954, https://doi.org/10.1007/s12011-020-02237-1

Zhang Y., He Y., Zhang D., Zhang M., Wang M.Y., Zhang Y., Ma T.Y., Chen J.H., 2018. Death of chondrocytes in Kashin-Beck disease: apoptosis, necrosis or necroptosis? Int. J. Exp. Pathol. 99, 312−322, https://doi.org/10.1111/iep.12297

Zhang Y., Li Z., He Y., Liu Y., Mi G., Chen J., 2022b. T-2 toxin induces articular cartilage damage by increasing the expression of MMP-13 via the TGF-β receptor pathway. Hum. Exp. Toxicol. 41, 9603271221075555, https://doi.org/10.1177/09603271221075555

Zhang Z.G., Fu F.D., Bian Y.S. et al., 2022c. Alpha-chaconine facilitates chondrocyte pyroptosis and nerve ingrowth to aggravate osteoarthritis progression by activating NF-κB signaling. J. Inflamm. Res. 15, 5873−5888, https://doi.org/10.2147/JIR.S382675

Zhou X.R., Yang H.J., Guan F., Xue S.H., Song D.Q., Chen J.H., Wang Z.L., 2015. T-2 toxin alters the levels of collagen II and its regulatory enzymes MMPs/TIMP-1 in a low-selenium rat model of Kashin-Beck disease. Biol. Trace Elem. Res. 169, 237−246, https://doi.org/10.1007/s12011-015-0408-2